Moroccan Journal of Chemistry
ISSN: 2351-812X
http://revues.imist.ma/?journal=morjchem&page=login
H. Hadki & al. / Mor. J. Chem. 9 N°2 (2021) 198-209

DFT and Molecular docking study of natural molecules proposed for COVID-19 treatment

H. El Hadki[(a)]*, A. El Hadki[(a)], R. Tazi[(a)], N. Komiha[(a)], A. Zrineh[(a)], S. El Hajjaji[(a)], O.K. Kabbaj[(a)]

[(a)] CERNE2D: Laboratory of Spectroscopy, Molecular Modelling, Materials, Nanomaterials, Water and Environment (LS3MN2E) - Faculty of Sciences - University Mohammed V, Rabat – Morocco

** Corresponding author:*
hamza.hadk@gmail.com
Received 16 Jun 2020,
Revised 18 Jan 2021,
Accepted 08 April 2021

Abstract

Emergence and spread of corona virus disease 2019 (COVID-19), caused by severe respiratory syndrome coronavirus, is considered a public health emergency threatening global health systems, as of June, 2020, It caused a cumulative total of 9,033,423 confirmed cases and more than 469,539 deaths across 215 countries, person to-person transmission has being identified as the route for spreading. So far, the lack of effective vaccines for the treatment or prevention of Covid-19 has further worsened the situation. In this context, the present study aims to assess whether naturally occurring components have an antiviral effect via a computational modeling approach. Density Functional theory (DFT) was performed to estimate the kinetic parameters, frontier molecular orbitals, molecular electrostatic potential as well as chemical reactivity descriptors of various ligands. The results revealed that Crocin and Digitoxigenin exhibited a potential applicant with the lowest resistance to electronic charge transfer with a chemical hardness of 2.19eV and 2.96eV respectively, as well as the lowest HOMO-LUMO difference. In addition to the DFT calculation, a docking simulation study was conducted on the SARS-CoV-2 base protease (PDB: 6LU7) to determine the binding affinity of ligands. The findings show that Crocin exhibits the lowest binding energy of -8.1 Kcal/mol and may be a good inhibitor of CoV-2-SARS compared to hydroxychloroquine and chloroquine, which have a binding affinity of -5.4 and -4.9 Kcal/mol, respectively. The high binding affinity of L3 was assigned to the existence of 14 hydrogen bonds connecting the ligand to the critical amino acid residues of the receptor.

Keywords: *DFT study, Molecular Docking, CoV-2019, Natural herbal medicine, hydroxychloroquine.*

1. Introduction

Toward the end of December 2019, a pneumonia associated with newly identified coronavirus disease (COVID-19) has emerged as a serious threat for global health systems [1], the causative viral agent of the recently emerged respiratory disease was identified to be the pathogenic severe acute respiratory syndrome coronavirus 2 (SARS-CoV-2) [2]. This pathology was First reported during an outbreak in the city of Wuhan, in the China region of Hubei, and then got rapidly and dynamically spread to other Asian countries, and subsequently to all corners of the world in an exponential trend within a matter of weeks [3,4], At the time of writing, a cumulative total of 9,033,423 cases of COVID-19 have been confirmed across 215 countries, resulting in more than 469,539 deaths [5], The alarming levels of spread, high morbidity and mortality forced the Director-General of the World Health Organization (WHO) to formally declare ,in the middle of March 2020, the corona virus disease-19 as a pandemic [6,7]. Currently, lack of specific vaccines and custom-made antiviral agents for the treatment of this deadly virus remains a major constraint, which is further aggravating the situation. Unfortunately, development of these treatments is a hugely time- consuming and arduous process as it involves clinical trials to prove the efficacy and safety of the new drugs. Till date, various therapeutic strategies are currently being considered a short-term solution for the management of the ongoing COVID–19 pandemic, including the repurposing of available and approved drugs, that includes Hydroxychloroquine, an FDA-approved drug for malaria [8,9]. It has been reported previously that chloroquine and hydroxychloroquine can inhibit coronavirus (COVID-19) by varying the pH at the surface of the cell membrane [10] and Dexamethasone, a corticosteroid drug used primarily for their anti-inflammatory effect. At high doses, they decrease the immune response. Hence, great attention has been paid to adjuvant therapies including the application of herbal treatment and natural products as they provide enormous structural and chemical diversity, as well as a well-established pharmacodynamics and pharmacokinetic properties, this is supported by the fact that around 45% of commercialized medicine have originated from natural compounds [11,12]. In this study, a functional density theory and molecular docking were performed on chloroquine, hydroxychloroquine, Dexamethasone, Lamivudine and 6 compounds extracted from different Moroccan medicinal plants to determine the active compounds against the coronavirus, thus providing a reference for the effective development of new drugs.

2. Materials and methods

*2.1. **DFT Calculation***

A complete optimization of all inhibitor compounds was conducted using the B3LYP exchange-correlation functional together with the LANL2DZ basis set in the gas phase using Berny's analytical gradient algorithm implemented in Gaussian 09 software package [13]. The nature of the stationary geometries was analyzed by a frequency calculation in order to verify the existence of no imaginary frequency. To identify the most favorable reactive site of ligands, local chemical reactivity Fukui function was calculated by means of NBO (Natural Bond Orbital) [14] using the following equations:

$$f_k^+ = q_k^{N+1} - q_k^N$$

$$f_k^- = q_k^N - q_k^{N-1}$$

where k, N and q correspond respectively to atomic number, number of electrons and net charge. The optimized molecular structures were visualized using GaussView graphical interface [15].

*2.2. **Molecular docking***

*2.2.1. **Ligands and protein preparation***

The three-dimensional (3D) structures of all inhibitor molecules studied were optimized by means of density functional theory as mentioned above and reported in figure1. A database where all ligands were converted to their 3D structures was created and used as an automatic dock input. The crystal structure of COVID-19 main protease in complex with an inhibitor N3 (PDB ID: 6LU7) [16] was obtained from RCSB PDB database. Crystallized ligands along with water molecules were omitted from the PDB file and polar hydrogen atoms were added to transmit electric charge and magnetic field.

*2.2.2. **Molecular docking protocol***

In order to determine the binding mechanism and interaction of the selected chemical species with the target, docking studies were conducted using Autodock/vina program [17]. The pdbqt files of the receptor protein and the different ligands as well as the grid box setting at the active receptor site, were performed using the Autodock 1.5.4 tools from MGL Tools. The limits of the grid size corresponding to the receiver pocket along the X, Y and Z axes (x = -29.128, y =8.134, z = 50.148) have been scaled to 40 Å with a spacing of 0.375 Å to allow adequate binding flexibility at the docked sites. The structure of COVID-19 was considered as a fixed entity while the ligands were kept flexible to obtain the best possible conformation. The generated docking solutions were grouped together and those corresponding to an average root square deviation value (RMSD) less than 1.0 Å were accounted. The binding conformation of the ligands with the lowest binding affinity was considered to be the most stable. Bonding interactions between ligand atom and active site residues were evaluated [18]. The results were examined using the Discovery 2016 studio Visualizer [19] and PyMol Molecular Graphics System [20].

3. Result and Discussion

*3.1. **DFT Study***

Quantum chemistry calculations using functional density theory were performed to investigate the effect of molecular structure on the interaction process of various ligands on the complex structure of the COVID-19 protein. The optimized molecular structures, the frontier molecular orbitals, the chemical reactivity descriptors and the molecular electrostatic potential maps of all investigated compounds are developed bellow.

Compounds	Structure	Origin
Camphene (L1)	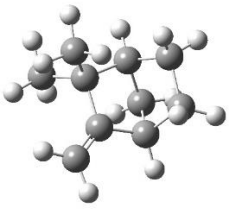	Thymelea Tartonraira
Chloroquine (L2)	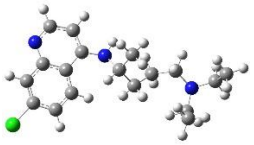	Drug
Crocin (L3)	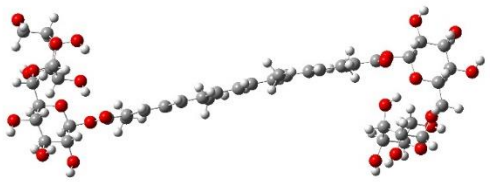	Crocus Sativus L

Digitoxigenine (L4)	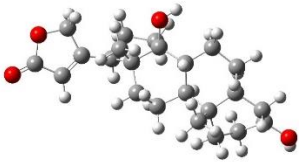	Nerium Oleander
Estragol (L5)	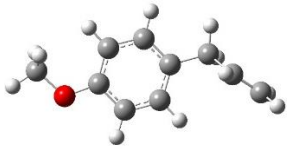	Foeniculum Vulgare
β-Eudesmol (L6)	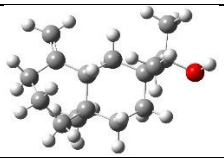	Lauris Nobilis L
Hydroxychloroquine (L7)	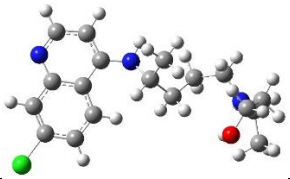	Drug
Lamivudin (L8)	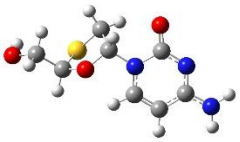	Drug
Picrocrocin (L9)	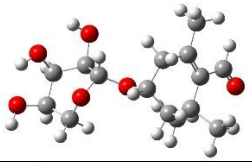	Crocus Sativus L
Dexamethasone (L10)	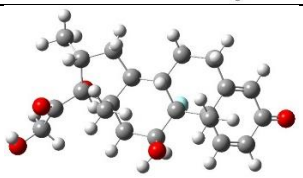	Drug

Figure 1. Optimized geometrical structures and origin of various ligands

3.1.1. ***Kinetic study***

Theoretical calculations were carried out in the gas phase using the B3LYP/LANL2DZ method. We found that all optimal compounds are stable and no imaginary frequencies were detected. The estimated DFT calculations for total energy, thermal parameters, dipole moment and polarizability of the various ligands are summarized in Table 1. The analysis of the data reveals that the stability of the studied compounds is as the following order L3 < L10 < L4 < L9 < L7 < L2 < L8 < L6 < L5 <L1. It can be noted that the ligand L3 corresponding to the Crocin is the most stable and therefore the least reactive. The high dipole moment of hydroxychloroquine (L7) may reflect their favorable binding position in relation to the protein

3.1.2. ***Frontier Molecular Orbitals***

The characterization of the frontier molecular orbitals (FMOs) plays an influential role in chemical stability since they reflect the reactivity as well as the mode of interaction of inhibitor with other molecules. Indeed, FMOs can provide realistic qualitative information on the susceptibility of an electron transfer from HOMO to LUMO and highly energetic HOMO-LUMO gap of a compound means its resistance to accept and donate electron leading to electronic stability in

the system [21]. The energies of the HOMOs and LUMOs of the studied compounds and their energetic difference ΔE are reported in Table 2. As shown in Table 2, the Camphene ligands (L1) and β-Eudesmol (L6) have the largest HOMO-LUMO energy gap involving a great stability. For hydroxychloroquine (L7) and Dexamethasone (L10), this parameter is higher so these ligands are less reactive towards the protein target.

Table 1. Total energy in (a.u), Gibbs free energy in (a.u), dipole moment μ in (Debye) and polarizability α in ($Bohr^3$)

Compounds	E	G	μ	α
L1	-390.613944	-390.408570	0.75	97.54
L2	-880.611584	-880.249660	6.91	228.44
L3	-3519.967595	-3519.001319	7.78	915.12
L4	-1196.968174	-1196.491542	8.07	239.30
L5	-463.411076	-463.253260	1.84	107.57
L6	-662.361147	-662.016815	1.71	152.43
L7	-955.825823	-955.460017	8.74	231.06
L8	-711.389600	-711.229784	4.65	128.43
L9	-1037.204575	-1036.871334	5.49	171.21
L10	-1331.557461	-1331.129644	4.46	236.15

Table 2. OMF's energy of investigated compounds

Compounds	E_{HOMO}	E_{LUMO}	ΔE
L1	-6.42	0.52	6.94
L2	-5.27	-1.57	3.69
L3	-5.43	-3.24	2.18
L4	-4.45	-1.49	2.95
L5	-5.90	-0.32	5.59
L6	-6.39	0.50	6.89
L7	-5.89	-1.57	4.32
L8	-6.56	-1.34	5.23
L9	-6.48	-1.60	4.88
L10	-6.60	-1.93	4.66

*3.1.3. **Chemical reactivity descriptors***

Based on previous data, we have identified and reported in Table 3 several DFT based global reactivity descriptors (CDFT) such as electronic chemical potential (μ), chemical hardness (η) and global electrophilic index (ω) using the following expression [22]:

$$\mu = \frac{(E_{HOMO} + E_{LUMO})}{2}$$

$$\eta = E_{LUMO} - E_{HOMO}$$

$$\omega = \frac{\mu^2}{2\eta}$$

Table 3. Global reactivity descriptors of investigated compounds

Compounds	E_{HOMO}	E_{LUMO}	μ	η	ω
L1	-6.42	0.52	-2.95	6.94	0.63
L2	-5.27	-1.57	-3.42	3.70	1.58
L3	-5.43	-3.24	-4.34	2.19	4.29
L4	-4.45	-1.49	-2.97	2.96	1.49
L5	-5.90	-0.32	-3.11	5.58	0.87
L6	-6.39	0.50	-2.95	6.89	0.63
L7	-5.89	-1.57	-3.73	4.32	1.61
L8	-6.56	-1.34	-3.95	5.22	1.49
L9	-6.48	-1.60	-4.04	4.88	1.67
L10	-6.60	-1.93	-4.27	4.67	1.95

Chemical hardness is employed as a tool for interpreting chemical reactivity and to measure a system resistance to a transfer of charge. The lower the values, the more likely the system is to be subject to electron transfer [23-25]. From the data displayed in table 3, we noticed that L1 and L6, recording the highest value respectively at 6.94eV and 6.89eV, are the most resistant compound to an electronic transfer thus the most stable in agreement with the previous finding, while the ligands L3 and L4 are the least resistant respectively at 2.19eV and 2.96eV. In order to predict the most favorable electrophilic and nucleophilic center of our compounds, local chemical reactivity Fukui function were analyzed, Figure 2 shows the 3D representation of the electrophilic (f_k^+) and nucleophilic (f_k^-) most favorable sites. We limit our study to the five most reactive ligand namely L3, L4, L2, L7 and L10.

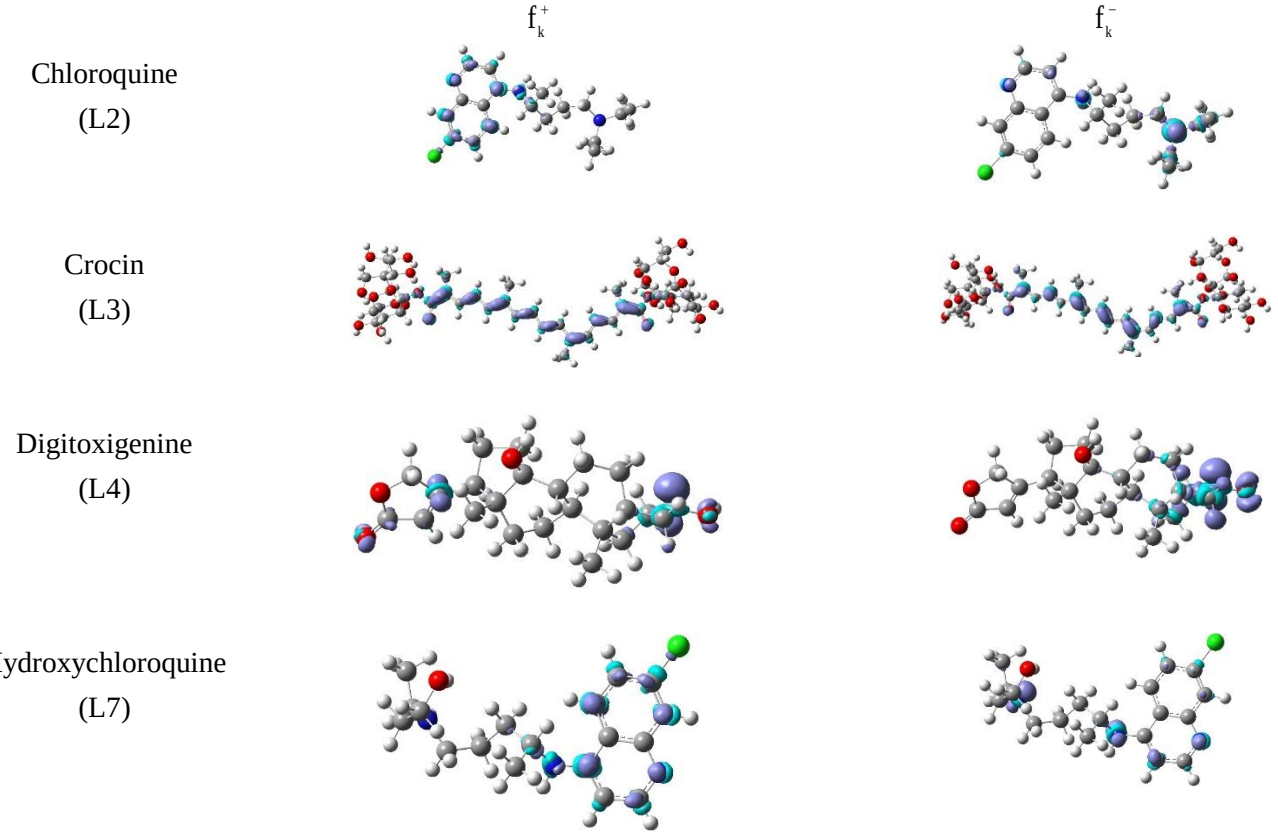

Dexamethasone (L10)

Figure 2. 3D representation of Fukui function for the selected ligands

*3.1.4. **Molecular electrostatic potential (MEP)***

Electrostatic attraction between molecules would be one of the important driving forces for complex formation. It is a powerful measure for estimating the reactivity of a compound to electrophilic and nucleophilic attacks. To address the preceding assumption, and to further refine the findings, DFT calculations of the electrostatic potential for selected ligands were performed. The results are visualized in figure 3.

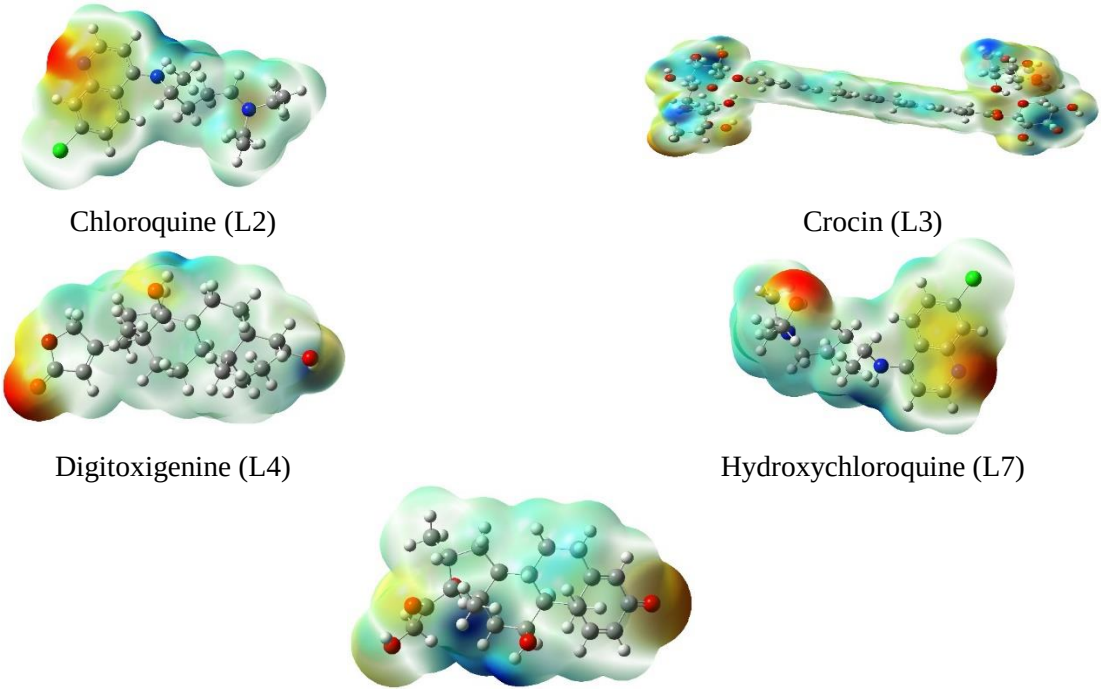

Figure 3. Molecular electrostatic potentials (MEP) of selected ligands

The analysis of the data indicates that for all ligands, the region of low electrostatic potential (red zone), characterized by an abundance of electrons, is mainly localized on oxygen or nitrogen atoms; this is certainly due to the high electronegativity of these atoms. As for the positive electrostatic potentials (blue zone) characterized by a lack of electrons are localized on the hydrogen atoms of the functional groups.

*3.2. **Molecular docking***

In the following, demonstration of the model describing the docking of 10 molecules into the complex structures of the COVID-19 protein. The docking results calculations of all ligands with the COVID-19 target are listed in Table 4. The molecules with the lowest binding energy of the docking score were selected as the best ligand and inhibited the target receptor because the lowest binding energy corresponds to a higher binding affinity, a larger surface area and the most hydrogen bonds [18]. As shown in table 4, docking results revealed that among the studied compounds, Crocin (L3), Digitoxigenine (L4) and Dexamethasone (L10) are the three compounds to have the best binding ability toward the COVID-19 protein, specifically, the L3 has the strongest inhibitory effects on the PDB6LU7 protein in the COVID-19

with a docking result of -8.1 Kcal/mol. Analysis of the key binding sites of the docked complex PDB6LU7 showed that Crocin ligand formed very strong interactions with the amino acids SER139, VAL125, SER123, THR199, ASN238, ASP197, ASN133, the interactions mainly took place with the molecule groups containing oxygen, in addition to the hydrogen bonds, Crocin ligand interacted with several receptor with different hydrophobic interactions. For L4, the analysis revealed a binding score of -7.4 Kcal/mol and an interaction with the receptor with various hydrophobic interactions in addition to two hydrogens bonds with ARG131 and MET276, as for L10, a binding score of -7.7 Kcal/mol, we note the formation of 2 interactions with LEU287 amino acid.

Table 4. Binding affinities (Kcal/mol) of docked compounds using Autodock/vina.

Compounds	Binding Affinities (kcal/mol)	Distance from Best Mode	
		RMSD Lower Bound	RMSD Upper Bound
Camphene	-4.7	0.000	0.000
Chloroquine	-4.9	0.000	0.000
Crocin	-8.1	0.000	0.000
Digitoxigenine	-7.4	0.000	0.000
Estragol	-4.3	0.000	0.000
β-Eudesmol	-5.5	0.000	0.000
Hydroxychloroquine	-5.4	0.000	0.000
Lamivudin	-5.1	0.000	0.000
Picrocrocin	-5.8	0.000	0.000
Dexamethasone	-7.7	0.000	0.000

By comparing the aforementioned molecules with Hydroxychloroquine on the basis of the interaction energy criterion, we can note that the studied ligands might be better inhibitor candidate for the coronavirus (COVID-19). Indeed, the molecular docking results showed that Hydroxychloroquine (L7) exhibited a medium affinity of -5.4 Kcal/mol for the selected target and that L7 is combined to LYS102 and SER158 in the form of hydrogen bonds as well as one interaction between the π systems with PHE294 active site residue. All residues of the COVID-19 protein interface engaged in ligand binding are shown in Figures 4(a, b, c and d). A detailed 3D inhibitor- interface interactions are represented in Figure 5(a, b, c and d).

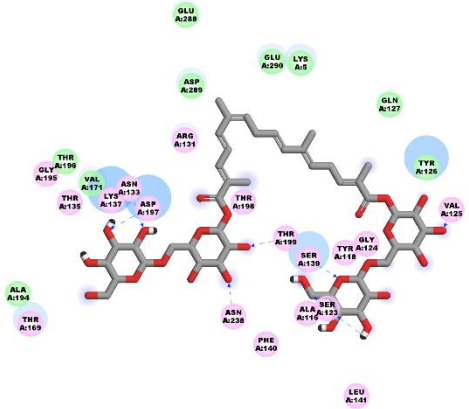

Figure 4a. 2D View of the binding conformation of the Crocin inhibitor at the active site of Coronavirus (COVID-19) spike protein

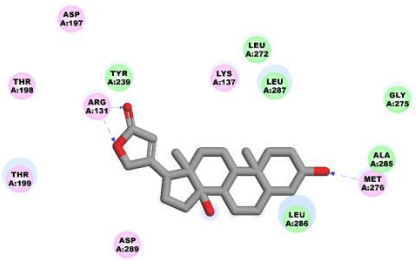

Figure 4b. 2D View of the binding conformation of the Digitoxigenine inhibitor at the active site of Coronavirus (COVID-19) spike protein

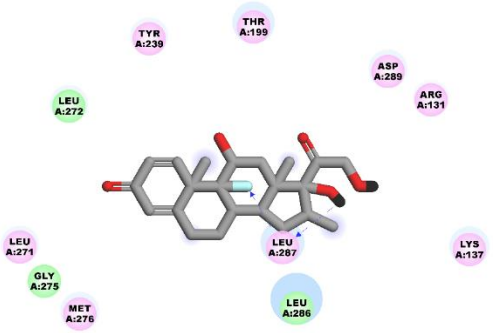

Figure 4c. 2D View of the binding conformation of the Dexamethasone inhibitor at the active site of Coronavirus (COVID-19) spike protein

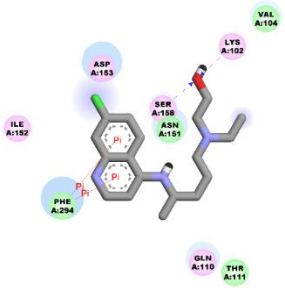

Figure 4d. 2D View of the binding conformation of the Hydroxychloroquine inhibitor at the active site of Coronavirus (COVID-19) spike protein

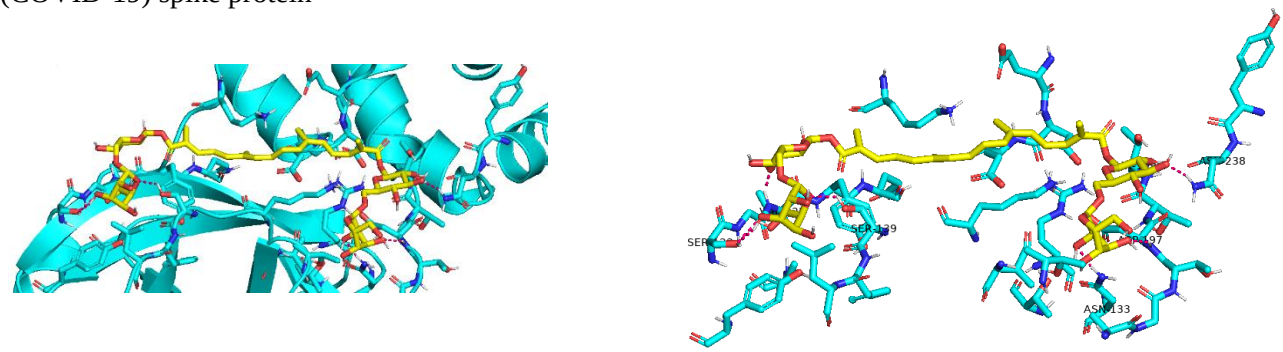

Figure 5a. 3D View of the binding conformation of the Crocin inhibitor at the active site of Coronavirus (2019-nCoV) spike protein

Figure 5b. 3D View of the binding conformation of the Digitoxigenine inhibitor at the active site of Coronavirus (2019-nCoV) spike protein

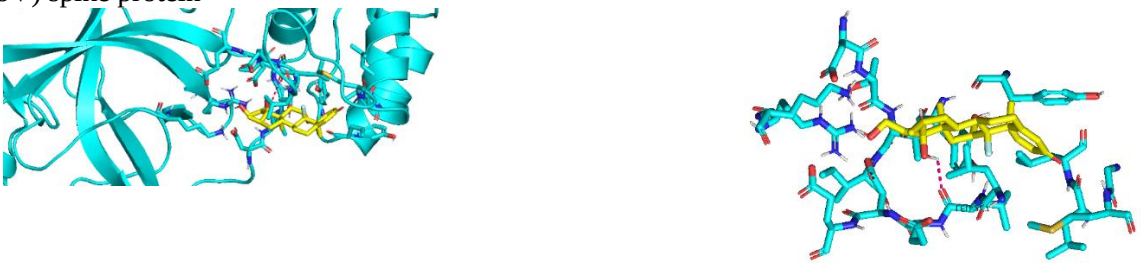

Figure 5c. 3D View of the binding conformation of the Dexamethasone inhibitor at the active site of Coronavirus (2019-nCoV) spike protein

Figure 5d. 3D View of the binding conformation of the Hydroxychloroquine inhibitor at the active site of Coronavirus (2019-nCoV) spike protein

In summary, after the analysis of the obtained results, the Crocin emerged as the most potent natural agent to treat COVID-19 compared to Hydroxychloroquine because of the presence of eight Hydrogen bonds interaction with the studied protein. All detailed docking results of Crocin ligand are displayed in table 5.

Table 5. docking results of Crocin ligands and the number of hydrogen bonds as well as interacting amino acids

Ligand	Binding energy (Kcal/mol)	Interacting residues	Types of bonds	Distance (Å)
Crocin	-8.1	ASN133	Hydrogen bond	2.1
		ASP197		2.4
		ASN238		2.1
		THR199		2.0
		SER139		2.2
		SER126		2.3 – 2.2
		VAL125		2.0

4. Conclusion

In this study, a density functional theory and molecular docking computation was adopted. The DFT results revealed that among the 10 initial ligands, Crocin (L3) and Digitoxigenine (L4) presented potential candidate being the least resistance to an electronic transfer of charge as well as the lowest HOMO-LUMO gap. In addition, the most electrophilic sites of these ligands are localized over nitrogen and oxygen atoms, which could be explained by the presence of the isolated electron pair on these atoms. The findings of the docking research were to investigate the mode of binding of these drugs to the crystal structure of COVID-19 main protease. The results highlighted that from the 6 compounds

extracted from different aromatic and medicinal plants, Crocin (L3) and Digitoxigenine (L4) had the highest affinity for the target receptor respectively at -8.1 Kcal/mol and 7.4 Kcal/mol. In addition, the binding affinity of Dexamethasone (L10) is lower when compared to the currently approved drugs, chloroquine (L2) and hydroxychloroquine (L7), which have respectively a binding affinity of -4.9 Kcal/mol and -5.4 Kcal/mol. Finally, natural constituents revealed to have potential antiviral agents against novel coronavirus.

Acknowledgment

We are thankful to the "Association Marocaine des Chimistes Théoriciens" (AMCT) for the programs.

References

[1] P. Zhou, X.-L. Yang, X.-G. Wang, B. Hu, L. Zhang, W. Zhang, H.-R. Si, Y. Zhu, B. Li, C.-L. Huang, H.-D. Chen, J. Chen, Y. Luo, H. Guo, R.-D. Jiang, M.-Q. Liu, Y. Chen, X.-R. Shen, X. Wang, *Nature.* , 579 (2020) 270–273.

[2] A. E. Gorbalenya, S. C. Baker, R. S. Baric, R. J. de Groot, C. Drosten, A. A. Gulyaeva, B. L. Haagmans, C. Lauber, A. M. Leontovich, B. W. Neuman, D. Penzar, S. Perlman, L. L. M. Poon, D. Samborskiy, I. A. Sidorov, I. Sola, J. Ziebuhr, *Microbiology.* , (2020).

[3] C. Huang, Y. Wang, X. Li, L. Ren, J. Zhao, Y. Hu, L. Zhang, G. Fan, J. Xu, X. Gu, Z. Cheng, T. Yu, J. Xia, Y. Wei, W. Wu, X. Xie, W. Yin, H. Li, M. Liu, *The Lancet.* , 395 (2020) 497–506.

[4] N. Zhu, D. Zhang, W. Wang, X. Li, B. Yang, J. Song, X. Zhao, B. Huang, W. Shi, R. Lu, P. Niu, F. Zhan, X. Ma, D. Wang, W. Xu, G. Wu, G. F. Gao, W. Tan, *N Engl J Med.* , 382 (2020) 727–733.

[5] World Health Organisation. Novel Coronavirus (2019-nCoV) Situation Reports; World Health Organisation: Geneva, Switzerland. (2020).

[6] B. McKay, J. Calfas, A. T Coronavirus Declared Pandemic by World Health Organization (2020).

[7] WHO WHO Director-General's Opening Remarks at the Media Briefing on COVID-19 World Health Organization (WHO) (2020).

[8] X. Yao, F. Ye, M. Zhang, C. Cui, B. Huang, P. Niu, X. Liu, L. Zhao, E. Dong, C. Song, S. Zhan, R. Lu, H. Li, W. Tan, D. Liu, *Clinical Infectious Diseases.* , (2020) ciaa237.

[9] J. Liu, R. Cao, M. Xu, X. Wang, H. Zhang, H. Hu, Y. Li, Z. Hu, W. Zhong, M. Wang, *Cell Discov.* , 6 (2020) 16-20.

[10] M. Grimstein, Y. Yang, X. Zhang, J. Grillo, S.-M. Huang, I. Zineh, Y. Wang, *Journal of Pharmaceutical Sciences.* , 108 (2019) 21–25.

[11] P. Gautret, J.-C. Lagier, P. Parola, V. T. Hoang, L. Meddeb, M. Mailhe, B. Doudier, J. Courjon, V. Giordanengo, V. E. Vieira, H. T. Dupont, S. Honoré, P. Colson, E. Chabrière, B. La Scola, J.-M. Rolain, P. Brouqui, D. Raoult, *International Journal of Antimicrobial Agents.* , (2020) 105949-105973.

[12] M. R. Mehra, S. S. Desai, F. Ruschitzka, A. N. Patel, *The Lancet.* , (2020) S0140673620311806.

[13] M. J. Frisch, G. W. Trucks, H. B. Schlegel, G. E. Scuseria, M. A. Robb, J. R. Cheeseman, G. Scalmani, V. Barone, G. A. Petersson, H. Nakatsuji, X. Li, M. Caricato, A. Marenich, J. Bloino, B. G. Janesko, R. Gomperts, B. Mennucci, H. P. Hratchian, J. V. Ortiz, A. F. Izmaylov, J. L. Sonnenberg, D. Williams-Young, F. Ding, F. Lipparini, F. Egidi, J. Goings, B. Peng, A. Petrone, T. Henderson, D. Ranasinghe, V. G. Zakrzewski, J. Gao, N. Rega, G. Zheng, W. Liang, M. Hada, M. Ehara, K. Toyota, R. Fukuda, J. Hasegawa, M. Ishida, T. Nakajima, Y. Honda, O. Kitao, H. Nakai, T. Vreven, K. Throssell, J. A. Montgomery, Jr., J. E. Peralta, F. Ogliaro, M. Bearpark, J. J. Heyd, E. Brothers, K. N. Kudin, V. N. Staroverov, T. Keith, R. Kobayashi, J. Normand, K. Raghavachari, A. Rendell, J. C. Burant, S. S. Iyengar, J. Tomasi, M. Cossi, J. M. Millam, M. Klene, C. Adamo, R. Cammi, J. W. Ochterski, R. L. Martin, K. Morokuma, O. Farkas, J. B. Foresman, and D. J. Fox, Gaussian 09, Revision A.02 Gaussian, Inc., Wallingford CT, (2016).

[14] A. E. Reed, L. A. Curtiss, F. Weinhold, *Chem Rev.* , 88 (1988) 899–926.
[15] R. Dennington, T. Keith and J. Millam, Semichem. Inc., Shawnee Mission, KS, (2009).
[16] X. Qiu, C. A. Janson, W. W. Smith, S. M. Green, P. McDevitt, K. Johanson, P. Carter, M. Hibbs, C. Lewis, A. Chalker, A. Fosberry, J. Lalonde, J. Berge, P. Brown, C. S. V. Houge-Frydrych, R. L. Jarvest, *Protein Sci.* , 10 (2001) 2008–2016.
[17] O. Trott, A. J. Olson, *J Comput Chem.* , 31 (2010) 455-461.
[18] X. Xu, P. Chen, J. Wang, J. Feng, H. Zhou, X. Li, W. Zhong, P. Hao, *Sci China Life Sci.* , 63 (2020) 457–460.
[19] P. Pilot, Dassault Systèmes BIOVIA, discovery studio modelling environment. Release, (2016).
[20] W. L. DeLano, *Protein Crystallogr.* , 40 (2002) 82–92.
[21] N. S. Venkataramanan, A. Suvitha, H. Mizuseki, Y. Kawazoe, *Int J Quantum Chem.* , 115 (2015) 1515–1525.
[22] H. El-Hadki, F. Hlimi, M. Salah, K. Marakchi, N. Komiha, O. K. Kabbaj, *Orient J Chem.* , 34 (2018) 2992–2997.
[23] K. Gupta, S. Giri, P. K. Chattaraj, *J Phys Org Chem.* , 26 (2013) 187–193.
[24] C. Morell, V. Labet, A. Grand, H. Chermette, *Phys Chem Chem Phys.* , 11 (2009) 3417-3423.